SERTS-97 MEASUREMENTS OF RELATIVE WAVELENGTH SHIFTS IN CORONAL EMISSION LINES ACROSS A SOLAR ACTIVE REGION

J. W. BROSIUS[1], R. J. THOMAS[2], J. M. DAVILA[2] and W. T. THOMPSON[3]

[1]*Raytheon ITSS, Code 682, NASA's GSFC, Greenbelt, MD 20771, U.S.A.*
(e-mail: brosius@comstoc.gsfc.nasa.gov)
[2]*Laboratory for Astronomy and Solar Physics, Code 682, NASA's GSFC, Greenbelt,*
MD 20771, U.S.A. (e-mails: thomas@jet.gsfc.nasa.gov; davila@lindsay.gsfc.nasa.gov)
[3]*SM&A, Code 682, NASA's GSFC, Greenbelt, MD 20771, U.S.A.*
(e-mail: thompson@orpheus.nascom.nasa.gov)

Abstract. We used slit spectra from the 18 November 1997 flight of Goddard Space Flight Center's Solar EUV Rocket Telescope and Spectrograph (SERTS-97) to measure relative wavelength shifts of coronal emission lines as a function of position across NOAA active region 8108. The shifts are measured *relative to* reference wavelengths derived from spectra of the region's nearby quiet surroundings (not necessarily at rest) because laboratory rest wavelengths for the coronal EUV lines have not been measured to sufficient accuracy for this work. An additional benefit to this approach is that any systematic uncertainties in the wavelength measurements are eliminated from the relative shifts by subtraction. We find statistically significant wavelength shifts between the spatially resolved active region slit spectra and the reference spectrum. For He II 303.78 Å the maximum measured relative red shift corresponds to a Doppler velocity $\sim +13$ km s^{-1}, and the maximum relative blue shift corresponds to a Doppler velocity ~ -3 km s^{-1}. For Si X 347.40 Å, Si XI 303.32 Å, Fe XIV 334.17 Å, and Fe XVI 335.40 Å the corresponding maximum relative Doppler velocities are $\sim +19$ and ~ -14, $\sim +23$ and ~ -7, $\sim +10$ and ~ -10, and $\sim +13$ and ~ -5 km s^{-1}, respectively. The active region appears to be divided into two different flow areas; hot coronal lines are predominantly red-shifted in the northern half and either blue-shifted or nearly un-shifted in the southern half. This may be evidence that material flows up from the southern part of the region, and down into the northern part. Qualitatively similar relative wavelength shifts and flow patterns are obtained with SOHO/CDS spectra.

1. Introduction

Red shifts in emission lines of Si IV, C IV, O IV, and N V from the lower solar transition region were first reported by Doschek, Feldman, and Bohlin (1976) using *Skylab* ultraviolet spectra of quiet Sun and coronal hole areas. Their largest measured shift implied a downflow velocity ~ 15 km s^{-1}. Wavelengths were measured in solar limb spectra and found to agree with rest values tabulated by Kelly and Palumbo (1973). No significant shift was observed in O V, the hottest ion in their sample. Feldman, Cohen, and Doschek (1982) extended this work to include active regions, measuring red shifts corresponding to downflow velocities between 4 and 17 km s^{-1}. Subsequent observations have both confirmed the net red shift of

the lower transition region lines and extended measurements of the phenomenon to higher temperatures (Dere, 1982; Dere, Bartoe, and Brueckner, 1984; Hassler, Rottman, and Orrall, 1991; Brekke 1993; Brekke, Hassler, and Wilhelm, 1997; Chae, Yun, and Poland, 1998; Brosius, Thomas, and Davila, 1999; Brynildsen *et al.*, 1999; Thompson and Brekke, 1999).

Dere (1982) used active region plage and sunspot observations obtained with the NRL High-Resolution Telescope and Spectrograph (HRTS) sounding rocket experiment to measure typical downflow velocities ~ 10 km s^{-1} at log $T \sim 5.0$, and to extend the observed red-shift phenomenon to O V (log $T \sim 5.37$). Dere, Bartoe, and Brueckner (1984) found an average red shift corresponding to 5 km s^{-1} in the quiet Sun using the two strong C IV resonance lines at 1548.2 and 1550.7 Å (log $T = 5.0$), while Brekke (1993) used HRTS spectra to measure average quiet-Sun red shifts ~ 8 km s^{-1} in O V lines. Hassler, Rottman, and Orrall (1991) conducted an in-flight wavelength calibration of the LASP EUV Coronal Spectrometer during a 1987 sounding rocket experiment, allowing them to directly measure wavelengths of observed solar lines against platinum lines of known wavelength generated on-board. The C IV line at 1548 Å and Fe II line at 1563 Å yielded net red shifts corresponding to Doppler velocities of 7.5 ± 1.0 km s^{-1} and 2.7 ± 1.5 km s^{-1}, respectively, in the quiet Sun. The Si II line at 1533 Å and Ne VIII line at 770 Å yielded no net red shifts. Brekke, Hassler, and Wilhelm (1997) and Chae, Yun, and Poland (1998) used the SUMER (Solar Ultraviolet Measurements of Emitted Radiation) spectrometer aboard the SOHO (Solar and Heliospheric Observatory) spacecraft to find systematic red shifts in transition region as well as low coronal lines, extending the temperature range of the phenomenon to O VI (log $T \sim 5.46$), Ne VIII (log $T \sim 5.80$), and Mg X (log $T \sim 6.05$). Some of these results must be viewed with caution, since, as Brekke, Hassler, and Wilhelm (1997) point out, conflicting reference wavelengths have been reported for O VI and Mg X. (The Mg X reference wavelength that they adopted, 624.95 Å from Kelly (1987), is given to only two decimal places rather than three or four, indicating the relative uncertainty in its value.) Finally, Chae, Yun, and Poland (1998) report that the Mg X line appears to be blended in the SUMER spectrum with an unknown first- or second-order component that can affect its derived centroid wavelength.

Unfortunately, the absolute rest wavelengths for coronal EUV lines are not well known. For example, the Kelly (1987) finding list and the Fuhr, Martin, and Wiese (1988) atomic parameter compilation both adopt wavelengths for almost all of their Fe XI–XV EUV lines from the solar observations of Behring *et al.* (1976) or Behring, Cohen, and Feldman (1972). Behring *et al.* (1976) obtained a full-Sun solar spectrum from 160 to 770 Å on photographic plates during a sounding rocket flight in 1973. Their wavelength scale is based entirely on the wavelengths of 10 strong reference lines of He I, He II, O III, O IV, O V, and Ne VII compiled in Kelly and Palumbo (1973). However, the O IV and O V ions used by Behring *et al.* (1976) to derive their wavelength calibration were later found to exhibit persistent red shifts in a variety of solar features (Doschek, Feldman, and Bohlin 1976;

Feldman, Cohen, and Doschek, 1982; Dere, 1982; Brekke, 1993; Brekke, Hassler, and Wilhelm, 1997). Further, Brekke, Hassler, and Wilhelm (1997) also found red shifts in lines of Ne VIII, formed at a similar temperature ($\log T \sim 5.80$) as the Ne VII line ($\log T \sim 5.71$) used as a wavelength standard by Behring *et al.* (1976). Thus the EUV wavelengths compiled by Kelly (1987) for lines of Fe XI, XII, XIII, XIV, and XV (as well as several other ions), many of which are adopted from the two Behring references, are not laboratory rest values but solar values likely affected by whatever mechanism produces the observed solar wavelength shifts. It is, therefore, problematic to use those wavelengths as references for measuring coronal Doppler velocities. To measure *absolute* wavelength shifts on the Sun it is essential to compare observed solar wavelengths with accurate (to, say, three decimal places) laboratory rest wavelengths. An absence of the latter necessitates the measurement of *relative* wavelength shifts in the present work. Improved laboratory and/or theoretical values for EUV wavelengths from coronal ions would be extremely valuable.

Brosius, Thomas, and Davila (1999) used 170–340 Å spectra of NOAA region 7870 and its environs (its 'edge') obtained with SERTS-95 to measure relative wavelength shifts of coronal emission lines from various ion species, including He II, Si XI, and Fe X–XVI. (Achour *et al.* (1995) applied a similar approach to measure transition region differential red shifts between an active region and its quieter surroundings using HRTS spectra.) The average 'edge' spectrum was used to provide reference wavelengths against which to measure relative shifts in the active region. The lines of He II at 303.78 Å, Fe XII at 193.51 Å, Fe XIII at 202.05 Å, Fe XIV at 211.33 Å, Fe XV at 284.15 Å, and Fe XVI at 335.41 Å were used for measuring spatial variations of the relative wavelength shifts across the region because all of these lines are free from known blends in the SERTS-95 spectra and are either intrinsically strong or near the SERTS-95 peak sensitivity. The iron ions are the hottest ions ever used for this type of analysis. All six lines reveal statistically significant spatial variations in their measured relative wavelength shifts in the active region core, including mixtures of blue shifts and red shifts (each with maximum values corresponding to relative Doppler velocities $\sim$ 15 km s^{-1}), indicating a dynamic, turbulent corona. For each of these lines we calculated intensity-weighted relative Doppler velocities from wavelength shifts in the spatially averaged core spectrum, obtaining values of $+5.8 \pm 0.6$ km s^{-1} for He II, $+5.7 \pm 0.9$ km s^{-1} for Fe XII, $+0.4 \pm 0.7$ km s^{-1} for Fe XIII, -2.1 ± 1.0 km s^{-1} for Fe XIV, $+0.8 \pm 0.8$ km s^{-1} for Fe XV, and -1.1 ± 0.5 km s^{-1} for Fe XVI. Combining the above six lines with several additional ones that are strong enough in both the edge and average core spectra to provide reliable centroid measurements, we found statistically significant net relative red shifts for lines of He II, Fe X, Fe XI, and Fe XII; lines of Fe XIII and Fe XV show no significant shift while lines of Si XI, Fe XIV, and Fe XVI show a small net relative blue shift.

In the present work we apply a similar technique to that used by Brosius, Thomas, and Davila (1999) to measure *relative* Doppler velocities between an

active region and its quiet surroundings. Section 2 describes the SERTS instrument flown in 1997 (SERTS-97), Section 3 presents the solar observations, Section 4 provides wavelength shift measurements, Section 5 discusses implications of the measured shifts, and Section 6 summarizes our conclusions.

2. The SERTS-97 Instrument

The version of SERTS flown on 18 November 1997 recorded spectrographic data on a CCD-intensified detector over the wavelength range 297.5–353.5 Å with a spectral resolution (instrumental FWHM) of 115 mÅ. It incorporated the same multi-layer-coated toroidal diffraction grating that was flown in 1991 and 1993 (Brosius *et al.*, 1996), which enhanced the instrumental sensitivity in this wavelength range over that of a standard gold-coated grating by factors up to nine. The spatial resolution was about 7 arc sec. SERTS-97 simultaneously recorded high resolution spectra along a 6 arc min slit, and spectroheliograms of two 3 arc min × 8.5 arc min areas on each end of the slit. See Figure 1.

An end-to-end radiometric calibration of the rocket instrument was carried out at Rutherford-Appleton Laboratory in the same facility used to characterize the CDS experiment on SOHO, and using the same EUV light source recently re-calibrated by PTB against the BESSY synchrotron. SERTS-97 has been used to carry out an intensity cross-calibration with SOHO/CDS, one of the major objectives of this flight (Thomas *et al.*, 1999).

Pre- and post-flight wavelength calibrations were carried out at GSFC using EUV spectra of a hollow-cathode gas-discharge lamp emitting He II and Ne II lines with rest wavelengths known to better than 0.3 mÅ (Kaufman and Edlen, 1974). Although the wavelength scale itself remained constant for the pre- and post-flight laboratory wavelength calibrations, the zero point of this scale shifted slightly, indicating a small, constant offset between the in-flight wavelength scale and those measured in the laboratory. This translates into a systematic, constant error on every wavelength measured from each area observed on the Sun. Fortunately, systematic wavelength shifts introduced by this offset are eliminated (directly canceled) by treating *relative* wavelength shifts between two different physical areas. In other words, because wavelengths measured simultaneously in any two different areas on the Sun include the same systematic shift, this shift is eliminated by subtracting the two wavelengths. Because the He II line at 303.78 Å is strong in both the laboratory and the solar spectra, we use it as the reference wavelength on which the solar spectrum is fixed to the laboratory wavelength scale. Thus we set the He II wavelength in our solar reference spectrum equal to its laboratory rest wavelength of 303.7822 Å, and base all other wavelengths in the reference spectrum as well as in the spatially resolved active region spectra on this choice. Of course, this solar line could in fact be significantly Doppler-shifted relative to its rest value, which would impose an additional systematic offset on all measured
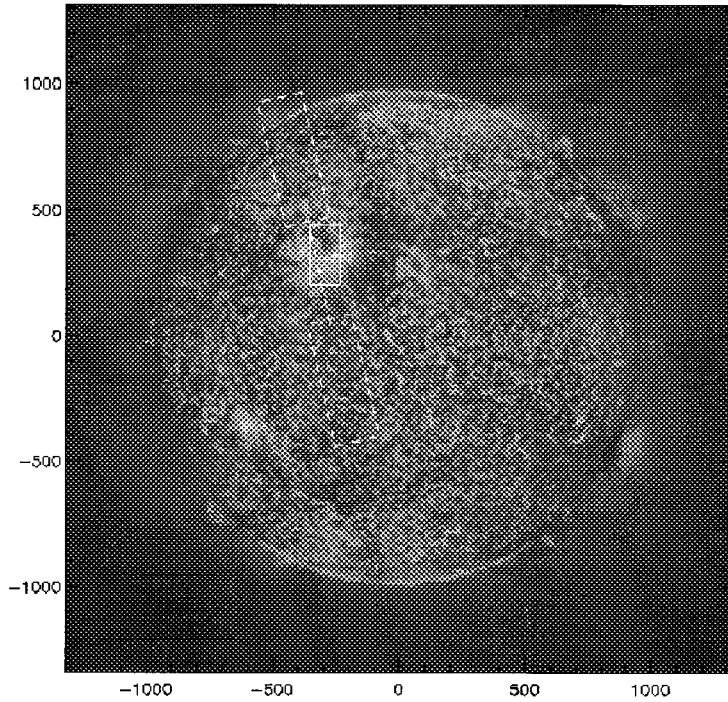
Figure 1. SOHO/EIT full-disk He II 304 Å image obtained during the SERTS rocket flight on 18 November 1997. The dashed rectangles outline the 3 arc min × 8.5 arc min areas within which SERTS spectroheliograms were obtained, and the dashed line connecting them shows the location of the 7 arc sec × 6 arc min SERTS slit. The solid rectangle shows the 2 arc min × 4 arc min CDS field of view, centered on NOAA region 8108. Solar north is at the top.

wavelengths. However, this offset too is eliminated from the *relative* wavelength shifts by subtraction.

3. Observations

SERTS was launched on a Terrier-boosted Black Brant rocket from White Sands, NM, at 19:35 UT on 18 November 1997. It reached a maximum altitude ∼ 330 km, and recorded spectrographic data for nearly 400 s. Spectroheliograms of NOAA active region 8108 (N21 E18) and slit spectra of quiet areas south and slightly west of this region were obtained in the first pointing position. Slit spectra of region 8108 and spectroheliograms of quiet areas to the northeast and southwest were obtained in the second. The absolute pointing of the instrument was derived by co-aligned the 3 arc min × 8.5 arc min He II 303.78 Å SERTS spectroheliograms with coordinated, full-disk He II 304 Å images from SOHO/EIT.

The 4 arc sec × 4 arc min CDS slit was used to raster spectral data over a 2 arc min × 4 arc min field of view. Spectral data were obtained in 16 wave bins,

Figure 2. SOHO/CDS Fe XVI 335 Å image of NOAA region 8108 showing the location of the SERTS-97 slit. The field of view is 2 arc min × 4 arc min, and solar north is at the top.

each covering 25 spectral pixels, for each 4 arc sec × 1.68 arc sec CDS spatial pixel. Fifteen of the wave bins are from NIS1, and one (covering the Si XI 303.32 and the He II 303.78 Å lines, seen in second order) is from NIS2. All wave bins include one or more lines observed by SERTS. We determined which CDS pixels mapped onto the SERTS slit, and used the coordinated spectral data to cross-calibrate CDS with SERTS (Thomas *et al.*, 1999) and to intercompare measured relative wavelength shifts.

SERTS spectra were recorded in 222 1.59-arc sec spatial pixels along the narrow slit, with each spatial pixel comprised of 2830 spectral elements. The 42 spatial pixels in the southernmost 67 arc sec (19%) of the slit in Figure 1 were used to obtain the average spectrum from the 'quiet surroundings'; this is the reference spectrum against which relative Doppler velocities in the active region are measured. For the active region, we treat only spectra from within the 221 arc sec segment (63% of the SERTS slit) within the CDS field of view. Figure 2 shows the Fe XVI 335.4 Å image of the active region from SOHO/CDS, with the SERTS slit superimposed for reference.

We examined the spatial variation of the He II 303.78 Å line centroid wavelength in laboratory spectra as well as in the quiet-Sun spectra from the first SERTS pointing position, and found that the wavelength varies systematically from one end of the slit to the other. The effect is somewhat more pronounced in the laboratory spectra than it is in the quiet-Sun spectra. We fit the systematic wavelength shift with a second order polynomial (see Figure 3), and used this polynomial to remove the systematic trend from the active region spectra in the second SERTS pointing position.
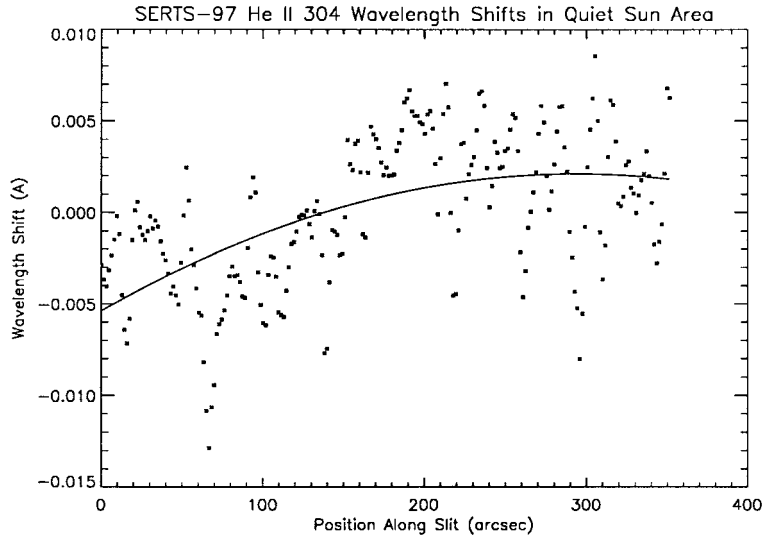
Figure 3. Quiet-Sun He II systematic wavelength shift along the SERTS-97 slit in pointing position 1, and the quadratic fit used to remove it.

4. Relative Wavelength Shifts

Gaussian fits to emission lines in the SERTS-97 spectra were carried out using a procedure similar to that described in Brosius *et al.* (1996) and Brosius, Davila, and Thomas (1998). Examples are shown in Figure 4. These fits yield the line centroid wavelength in Å, the total (integrated) intensity in erg cm^{-2} s^{-1} sr^{-1}, and the full width at half maximum intensity (FWHM) in mÅ, along with the 1-sigma standard deviation for each. Values of these quantities for five lines from the 'quiet surroundings' spectrum are given in Table I. All of these lines are relatively strong and free from known blends in the SERTS-97 spectra. T_{max} is the temperature that maximizes the fractional ion abundance in the available ionization equilibrium calculations. For iron, log T_{max} is derived from quadratic fits to the ionization equilibrium calculations of Arnaud and Raymond (1992); for other elements, it is derived from fits to similar calculations by Monsignori-Fossi (1992). The FWHM includes the instrumental width as well as both thermal and non-thermal contributions. The uncertainties listed for each wavelength are statistical only.

We fit Gaussian profiles to the lines listed in Table I for each of the 139 SERTS slit spatial pixels within the CDS field of view. Doppler shifts correspond to differences between fitted line profile centroids; Figure 5 shows examples of typical shifts observed. Figures 6–8 show the relative Doppler velocities derived between the 'quiet surroundings' and NOAA region 8108 as functions of position along the SERTS slit for He II 303.78 Å, Fe XIV 334.17 Å, and Fe XVI 335.40 Å. For reference we also display the total line intensity (in erg cm^{-2} s^{-1} sr^{-1}) in the top
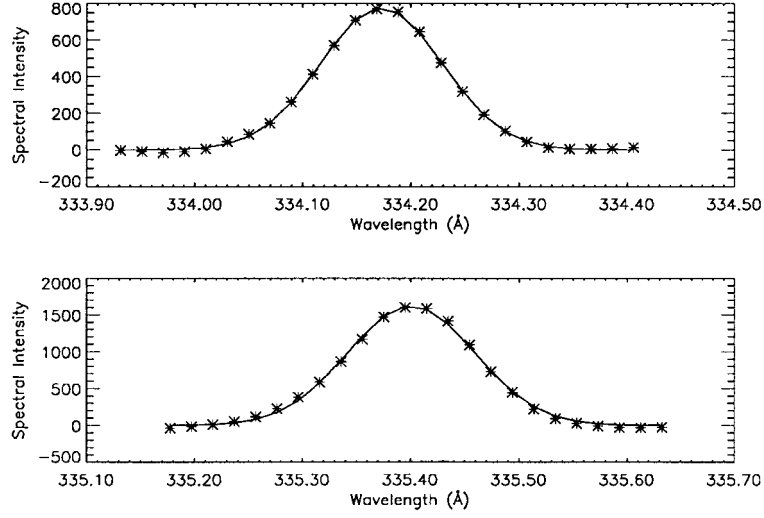
Figure 4. Gaussian fits to the Fe XIV 334.17 Å (*top*) and the Fe XVI 335.40 Å (*bottom*) lines from the SERTS-97 'quiet surroundings' spectrum. SERTS spectral data are shown as asterisks and the Gaussian fits are shown as solid lines. Spectral intensity is in erg cm^{-2} s^{-1} sr^{-1} $Å^{-1}$.

TABLE I

Spectral line data for the 'quiet surroundings' spectrum

Ion	$\log T_{max}$	Wavelength	Intensity	FWHM
He II	4.67	303.7822 ± 0.0005	8270 ± 929	144 ± 7
Si X	6.14	347.3984 ± 0.0011	102 ± 12	148 ± 8
Si XI	6.20	303.3188 ± 0.0012	643 ± 84	145 ± 8
Fe XIV	6.27	334.1728 ± 0.0004	110 ± 12	133 ± 7
Fe XVI	6.43	335.4006 ± 0.0007	239 ± 27	138 ± 7

frame of each figure. The first pixel in each figure corresponds to the southernmost SERTS slit pixel within the CDS field of view (see Figures 1 and 2). (The top frame in Figure 5 corresponds to $x \approx 75$ arc sec in Figure 7, and the bottom frame corresponds to $x \approx 190$ arc sec.) For He II the maximum measured relative red shift corresponds to a Doppler velocity $\sim +13$ km s^{-1}, and the maximum relative blue shift corresponds to a Doppler velocity ~ -3 km s^{-1}. For Fe XIV and Fe XVI the maximum relative red shifts correspond to Doppler velocities $\sim +10$ and $\sim +13$ km s^{-1}, respectively, while the maximum relative blue shifts correspond to Doppler velocities of ~ -10 and ~ -5 km s^{-1}, respectively. For Si X and Si XI the maximum relative red shifts correspond to Doppler velocities $\sim +19$ and $\sim +23$ km s^{-1}, and the maximum relative blue shifts correspond to ~ -14 and ~ -7.
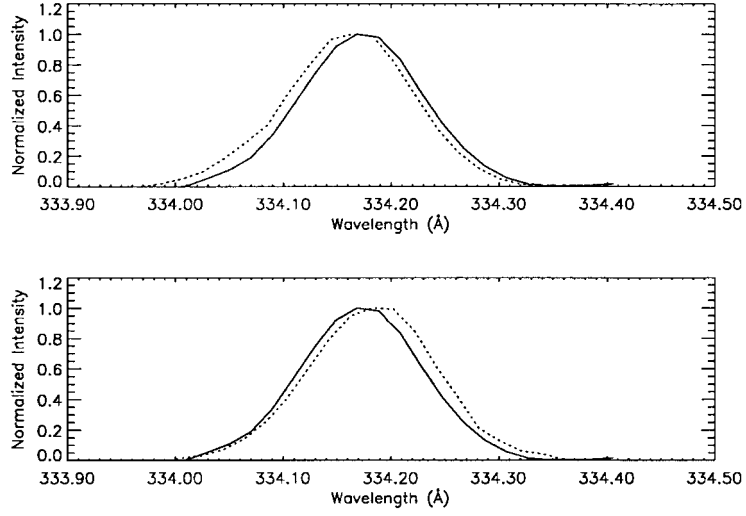
Figure 5. Fe XIV 334.17 Å line profile shifts between the 'quiet surroundings' (*solid*) and two different locations along the SERTS slit (*dotted*). We show normalized measured spectral data rather than Gaussian profile fits. The profile in the top frame is blue-shifted by a Doppler velocity corresponding to $\Delta V = -9.4 \pm 0.7$ km s^{-1}, and the profile in the bottom frame is red-shifted by a Doppler velocity corresponding to $\Delta V = +9.4 \pm 0.6$ km s^{-1}. Note that the entire profile moves symmetrically either blueward or redward of the reference profile.
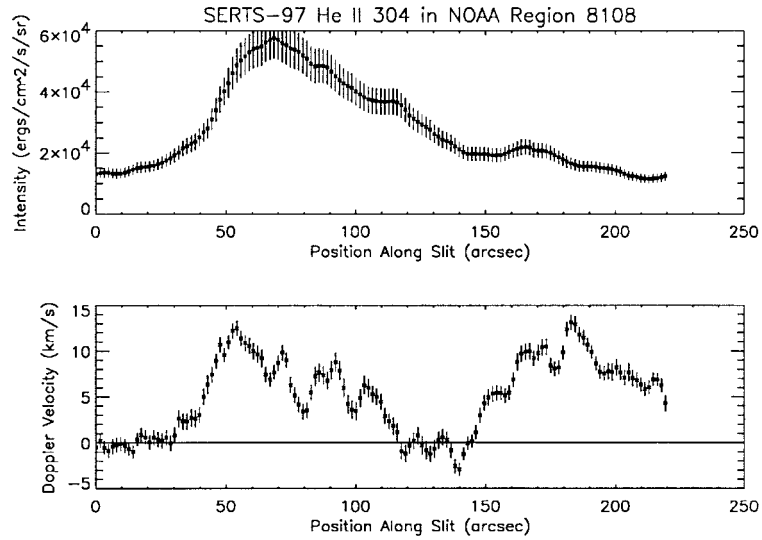

Figure 6. He II 303.78 Å line intensity (*top frame*) and relative Doppler velocity (*bottom frame*) as a function of position across region 8108.
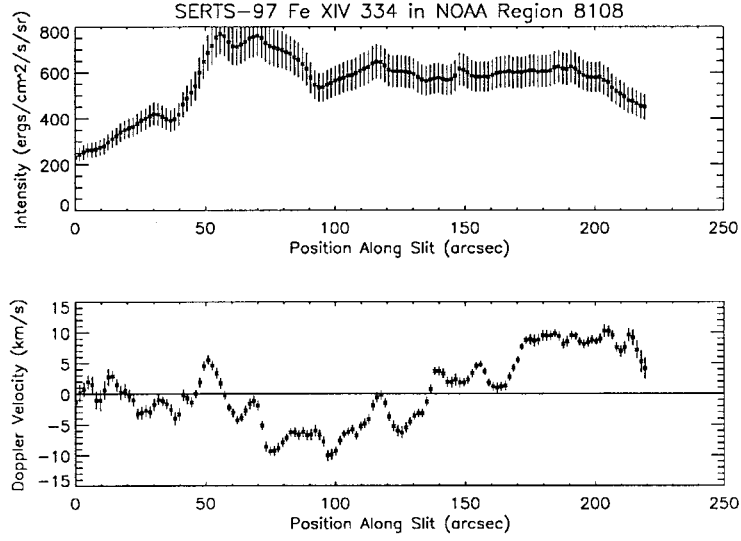
Figure 7. Fe XIV 334.17 Å line intensity (*top frame*) and relative Doppler velocity (*bottom frame*) as a function of position across region 8108.

Figure 9 shows relative wavelength shifts measured for He II 303.78 Å and Fe XVI 335.40 Å from spectra in the SOHO/CDS pixels that mapped onto the SERTS slit. Here, wavelength shifts are measured relative to (almost) average wavelengths rather than relative to the 'quiet surroundings' values. CDS wavelengths were corrected for spectral line tilt as described in Thompson and Brekke (1999). Note the qualitative similarity between these and the wavelength-shift variations seen in Figures 6 and 8.

5. Discussion

Brekke *et al.* (1997) argue that the Fe XVI resonance line at 335.41 Å, originally thought to be ideal for studying coronal mass motions with SOHO/CDS, is contaminated with a Mg VIII line at 335.23 Å and should not be used for coronal dynamical studies. Fortunately this is not a problem for SERTS since these two lines are well separated in SERTS spectra. The Mg VIII line is weak and not evident in either the active region or the 'quiet surroundings' spectra; however, it is easily visible in the quiet-Sun spectrum from the first pointing position.

Region 8108 appears to be divided into two different flow areas. The He II velocity pattern seen in Figure 6 suggests a southern half (from about 0 to 111 arc sec) wherein the maximum red shift corresponds to a Doppler velocity $\sim +12$ km s^{-1}, and a northern half (from about 111 to 221 arc sec) wherein the maximum red shift corresponds to a Doppler velocity $\sim +13$ km s^{-1}. Table II gives the (intensity-weighted) relative Doppler velocities for He II and five coronal ions in spatially
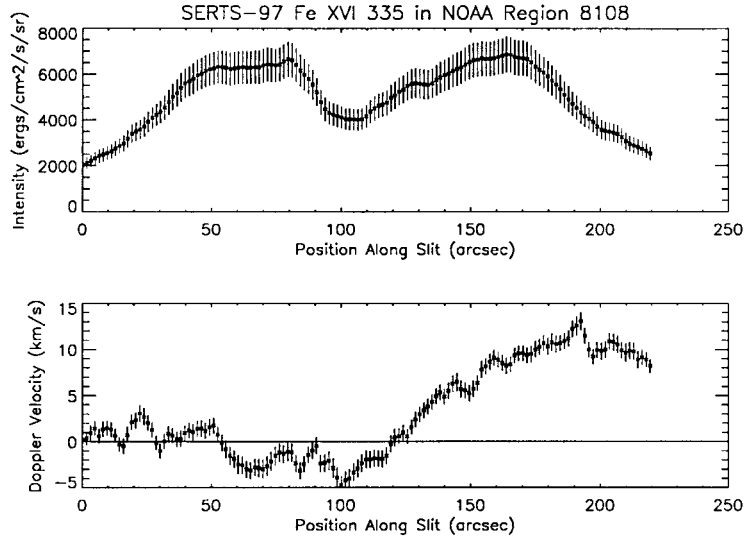
Figure 8. Fe XVI 335.40 Å line intensity (*top frame*) and relative Doppler velocity (*bottom frame*) as a function of position across region 8108.

TABLE II

Average relative Doppler velocities (km s^{-1}) in the southern and northern halves of region 8108

Ion	log T_{max}	ΔV_{south}	ΔV_{north}
He II	4.67	$+6.61 \pm 0.85$	$+4.34 \pm 0.77$
Si X	6.14	-2.24 ± 1.08	$+8.46 \pm 1.04$
Si XI	6.20	$+1.98 \pm 1.68$	$+7.31 \pm 1.37$
Fe XIII	6.20	-2.32 ± 1.05	$+5.25 \pm 1.00$
Fe XIV	6.27	-3.23 ± 0.57	$+3.50 \pm 0.51$
Fe XVI	6.43	-0.72 ± 0.88	$+6.88 \pm 0.82$

averaged spectra from the southern half and the northern half of the region. The hot coronal lines are predominantly red-shifted in the northern half and either blue-shifted or nearly unshifted in the southern half. This may be evidence that material flows up from the southern part of the region, and down into the northern part. An alternative explanation may be different velocities in adjacent loops, reflecting different heating and/or cooling histories. Teriaca, Erdelyi, and Doyle (1999) have interpreted red shifts of low to mid transition region lines and blue shifts of low coronal lines ($T > 6 \times 10^5$ K) observed in quiet-Sun spectra with SOHO/SUMER as signatures of nanoflares in the solar atmosphere.
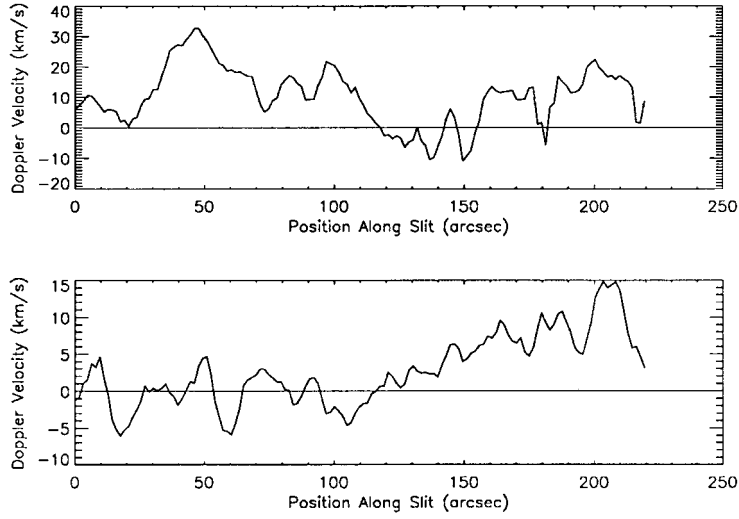
Figure 9. Relative Doppler velocities for He II 303.78 Å (*top*) and Fe XVI 335.40 Å (*bottom*) measured with SOHO/CDS, as a function of position across region 8108. Note that these exhibit the same general trends observed for the same lines with SERTS.

Although the CDS wavelength shifts are not measured relative to the same 'quiet surroundings' as those used for SERTS, both He II and Fe XVI show very similar trends to those seen with SERTS. Differences may be due to the different spatial resolutions. Also, although the CDS raster scanning was centered on the time of the SERTS flight, the scanning began before the flight and ended after it, so that the SERTS and CDS spectra are not everywhere exactly simultaneous.

6. Summary

We used SERTS-97 spectra to measure wavelength shifts of coronal emission lines in a solar active region *relative to* its quiet surroundings. This method removes any systematic uncertainties in the SERTS-97 wavelength calibration by cancellation, and circumvents the unavailability of reliable laboratory wavelengths for coronal emission lines by using lines from the 'quiet surroundings' spectrum as references. This means that we measure wavelength shifts of active region coronal emission lines not relative to a frame at rest (such as a laboratory frame), but relative to an area on the Sun which may itself be in motion. Statistically significant wavelength shifts between the spatially resolved active region slit spectra and the 'quiet surroundings' reference spectrum are found. For He II 303.78 Å the maximum measured relative red shift corresponds to a Doppler velocity $\sim +13$ km s^{-1}, and the maximum relative blue shift corresponds to a Doppler velocity ~ -3 km s^{-1}. For Fe XIV 334.17 Å the corresponding values are $\sim +10$ and ~ -10 km s^{-1}. For Fe XVI 335.40 Å the corresponding values are $\sim +13$ and ~ -5 km s^{-1}.

The active region appears to be divided into two different flow areas; hot coronal lines are predominantly red-shifted in the northern half and either blue-shifted or nearly un-shifted in the southern half. This may be evidence for material flows up from the southern part of the region, and down into the northern part. Qualitatively similar relative wavelength shifts (and flow patterns) are obtained with SOHO/CDS spectra that are found with SERTS spectra.

Acknowledgements

References

Achour, H., Brekke, P., Kjeldseth-Moe, O., and Maltby, P.: 1995, *Astrophys. J.* **453**, 945.

Arnaud, M. and Raymond, J.: 1992, *Astrophys. J.* **398**, 394.

Behring, W. E., Cohen, L., and Feldman, U.: 1972, *Astrophys. J.* **175**, 493.

Behring, W. E., Cohen, L., Feldman, U., and Doschek, G. A.: 1976, *Astrophys. J.* **203**, 521.

Brekke, P.: 1993, *Astrophys. J.* **408**, 735.

Brekke, P., Hassler, D. M., and Wilhelm, K.: 1997, *Solar Phys.* **175**, 349.

Brekke, P., Kjeldseth-Moe, O., and Harrison, R. A.: 1997, *Solar Phys.* **175**, 511.

Brekke, P., Kjeldseth-Moe, O., Brynildsen, N., Maltby, P., Haugan, S. V. H., Harrison, R. A., Thompson, W. T., and Pike, C. D.: 1997, *Solar Phys.* **170**, 163.

Brosius, J. W., Davila, J. M., and Thomas, R. J.: 1998, *Astrophys. J. Suppl.* **119**, 255.

Brosius, J. W., Thomas, R. J., and Davila, J. M.: 1999, *Astrophys. J.* **526**, 494.

Brosius, J. W., Davila, J. M., Thomas, R. J., and Monsignori-Fossi, B. C.: 1996, *Astrophys. J. Suppl.* **106**, 143.

Brynildsen, N., Maltby, P., Brekke, P., Haugan, S. V. H., and Kjeldseth-Moe, O.: 1999, *Solar Phys.* **186**, 141.

Chae, J., Yun, H. S., and Poland, A. I.: 1998, *Astrophys. J. Suppl.* **114**, 151.

Dere, K. P.: 1982, *Solar Phys.* **77**, 77.

Dere, K. P., Bartoe, J. -D. F., and Brueckner, G. E.: 1984, *Astrophys. J.* **281**, 870.

Doschek, G. A., Feldman, U., and Bohlin, J. D.: 1976, *Astrophys. J.* **205**, L177.

Feldman, U., Cohen, L., and Doschek, G. A.: 1982, *Astrophys. J.* **255**, 325.

Fuhr, J. R., Martin, G. A., and Wiese, W. L.: 1988, *J. Phys. Chem. Ref. Data* **17**, Supp. No. 4.

Hassler, D. M., Rottman, G. J., and Orrall, F. Q.: 1991, *Astrophys. J.* **372**, 710.

Kaufman, V., and Edlen, B.: 1974, *J. Phys. Chem. Ref. Data* **3**, 825.

Kelly, R. L.: 1987, *J. Phys. Chem. Ref. Data* **16**, Supp. No. 1 (Finding List).

Kelly, R. L., and Palumbo, L. J.: 1973, *NRL Report 7599*, (Naval Research Laboratory, Washington, D.C.

Monsignori-Fossi, B. C.: 1992, unpublished.

Teriaca, L., Erdelyi, R., and Doyle, J. G.: 1999, presented at the Monterey Workshop.

Thomas, R. J., Davila, J. M., Thompson, W. T., Kent, B. J., and Hollandt, J.: 1999, *Bull. Am. Astron. Soc.* **31**, 850.

Thompson, W. T. and Brekke, P.: 1999, presented at the Monterey Workshop.